DONOHUE, J. (1985). *Acta Cryst.* A**41**, 203-204.
HAMILTON, W. C. (1964). *Statistics in Physical Science.* New York: Ronald Press.
International Tables for X-ray Crystallography (1974). Vol. 1. Birmingham: Kynoch Press.
JABER, M., GUILHEM, J. & LOISELEUR, H. (1983). *Acta Cryst.* C**38**, 485-487.
LAWTON, S. L. (1973). *J. Appl. Cryst.* **6**, 309-316.
MARSH, R. E. (1983). *Acta Cryst.* C**39**, 1473.
MARSH, R. E. (1984). *Acta Cryst.* C**40**, 712.
MARSH, R. E. (1986). *Acta Cryst.* B**42**, 193-198.
MARSH, R. E. & HERBSTEIN, F. H. (1983). *Acta Cryst.* B**39**, 280-287.
MARSH, R. E. & SCHOMAKER, V. (1979). *Inorg. Chem.* **18**, 2331-2336.
MIGHELL, A. D., HIMES, V. L. & RODGERS, J. R. (1983). *Acta Cryst.* A**39**, 737-740.
SUGIO, S., MUJINO, H., HITAMURA, K., HAMADA, K., IKEHARA, M. & TOMITA, K. (1983). *Acta Cryst.* C**39**, 745-747.
WILSON, A. J. C. (1988). *Acta Cryst.* A**44**, 715-724.

Acta Cryst. (1990). A**46**, 730-734

Lorentz Factor for Oriented Samples in Powder Diffractometry

BY L. ZEVIN*

Laboratory for Crystallography, Katholieke Universiteit Leuven, Celestijnenlaan 200 C, B-3030 Heverlee, Belgium

(*Received* 12 *June* 1989; *accepted* 9 *April* 1990)

Abstract

Owing to axial divergence of the incident and diffracted beams in a powder diffractometer, poles of reflecting crystallites are spread over a significant angular range in the axial plane, normal to the focusing plane of the diffractometer. The probability for a crystallite to reflect X-rays depends on Bragg angle and on inclination of the pole to the focusing plane. In order to calculate the number of reflecting crystallites ('powder' supplement to the Lorentz factor) in an oriented sample, the orientation function of the crystallite must be multiplied by a probability function and integrated over the whole range of the pole's spreading caused by axial divergence. A probability function has been derived, and a 'powder' supplement to the Lorentz factor has been calculated for samples with various degrees of preferred orientation. It is shown that, in the 2θ range below 20°, the angular dependence of the Lorentz factor deviates considerably from the conventional form $(\sin\theta)^{-1}$. The required formulation is given for the intensity correction for low-angle reflections of oriented samples.

Introduction

The integrated intensity diffracted by the (hkl) plane of a randomly oriented non-absorbing powder specimen is most generally expressed (Azaroff, 1968) as

$$I = (KmH_c)/(8\pi R \sin\theta)QV, \qquad (1)$$

where K is the scale factor, m the multiplicity factor, H_c the length of the detector slit, R the diffractometer radius, Q the reflecting power per unit volume element and V the sample volume. The term $mH_c/(8\pi R \sin\theta)$ is proportional to the number of crystallites properly oriented so as to diffract X-rays into the detector slit of height H_c. The $(\sin\theta)^{-1}$ multiplier of this term, which emphasizes the θ dependence of the number of properly oriented crystallites, is of special interest here. In fact, $(\sin\theta)^{-1}$ may be regarded as the powder supplement to the regular single-crystal Lorentz factor equal to $(\sin 2\theta)^{-1}$ [included in Q in (1)], bringing the Lorentz factor for powders to its usual form $(\sin\theta \sin 2\theta)^{-1}$. In the case of an oriented powder sample, an additional term equal to the pole density in the direction of the diffraction vector P_0 must be introduced into (1) with the same aim of accounting for the number of correctly oriented crystallites.

Thus, the corrected intensity is given by

$$I_{cor} = K_0 Q V P_0 S_p, \qquad (2)$$

where K_0 includes the scale factor K, numerical constants, instrumental constants H_c and R, and multiplicity factor m from (1), and S_p is the angle-dependent powder supplement to the Lorentz factor. For a randomly oriented sample, $S_p = (\sin\theta)^{-1}$ and $P_0 = 1$.

Much effort has been devoted to acquiring P_0 values for various (hkl) planes using various approximations for the pole distribution function P (Roe & Krigbaum, 1964; Sturm & Lodding, 1968; Dollase, 1986). However, under certain experimental conditions, due to the finite size of the focal spot, sample and detector slit, crystallites with a considerable spread of orientations contribute to the integrated intensity of the

* Permanent address: The Institutes for Applied Research, Ben-Gurion University of the Negev, PO Box 1025, Beer-Sheva 84110, Israel.

0108-7673/90/090730-05$03.00

diffraction peak. This results in a substantial instrumental integration over the pole distribution function, which must be taken into account in the correction of the intensities of diffraction peaks. This effect is angle dependent, and in our further discussion we shall retain the term P_0 in (2) and all instrumental influence included in the value of the S_p powder supplement to the Lorentz factor. This matter has recently been treated by Reynolds (1986). However, he supposed that incident rays inclined to the focusing plane of the diffractometer illuminate a sample area with constant axial length. In fact, this length depends on the inclination angle, and Reynolds's calculations thus lead to a different formulation of the Lorentz factor and an estimation of it which is at variance with the results of the present paper.

The relevant theory is presented below with an outline of the experimental conditions for which instrumental integration must be taken into account during correction for preferred orientation.

Theory

We will discuss only the axial texture with the axis normal to the sample plane and along the diffraction vector. Our presentation is thus restricted to the Bragg–Brentano geometry where the diffraction vector and the sample normal are consistent. The condition imposed above is either naturally fulfilled for sedimented or compressed plate-like particles or can easily be achieved by specimen spinning around the sample normal. Under these conditions, the pole distribution is the function of a single variable - the latitudinal angle φ which we shall measure from the direction of the sample normal. The pole density distribution $P(\varphi)$ is subject to the normalization condition

$$2\pi \int_0^{\pi/2} P(\varphi)\sin\varphi \, d\varphi = \text{constant}. \qquad (3)$$

If we put $P(0) = 1$ for a randomly oriented sample, then constant $= 2\pi$ and

$$\int_0^{\pi/2} P(\varphi)\sin\varphi \, d\varphi = 1. \qquad (4)$$

Owing to the substantial axial divergence in powder diffractometers, the poles of diffracting crystallites are spread around the direction $\varphi = 0$. This matter was discussed in depth in the early years of X-ray diffractometry (Alexander, Klug & Kummer, 1948; de Wolff, 1958; Kheiker & Zevin, 1963). We shall use the same approach in evaluating integrated intensities in oriented samples. In contemporary powder diffractometers the focal spot, the irradiated part of the specimen and the receiving slit are of approximately equal height $H = 10$–12 mm. We consider X-rays diffracted by crystallites near the edge point of the sample P_1 (Fig. 1).

Suppose that an X-ray from the edge point of the focus F_1 strikes the sample at point P_1 and is reflected to the edge point of the detector slit C_1. The pole of reflecting crystallite P_1N_1 is coplanar with F_1P_1 and C_1P_1 and its inclination to the focusing plane (XY plane in Fig. 1) is zero ($\varphi = 0$). Consider now an X-ray from another edge point of the focus F_2 striking the same sample point P_1 and reflecting to point C_2 of the receiving slit. The pole of the reflecting crystallite P_1N_2 has maximal inclination to the focusing plane φ_{max}, where

$$\varphi_{max} = \arcsin\,[H/(R^2 + H^2)^{1/2}\sin\theta] \simeq \arcsin\,(H/R\sin\theta). \qquad (5)$$

It must be emphasized that a crystallite with various pole orientations between $\varphi = 0$ and $\varphi = \varphi_{max}$ will reflect X-rays consecutively and not simultaneously. Indeed, if reflection conditions are fulfilled for a crystallite with a pole orientation P_1N_2 (Fig. 1), they do not occur for a crystallite with pole $P_1N_1(\varphi = 0)$, because the angle $\beta \neq \theta$. However, during the diffractometer scan, reflection conditions will be fulfilled consecutively for all crystallites with pole orientation between $0 \leq \varphi \leq \varphi_{max}$, and all of them will contribute to the integrated intensity of the diffraction peak. However, the frequency of the different pole orientations is not constant and depends on angle φ. Consider a reflecting crystallite at an arbitrary point P_3 with coordinate Z for which the pole to reflecting

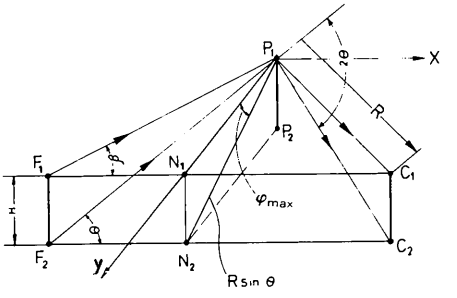

Fig. 1. Three-dimensional view of diffractometer geometry. F_1F_2 focal line; P_1P_2 sample; C_1C_2 detector slit. The axially divergent ray $F_2P_1C_2$ represents diffraction from a crystallite with pole P_1N_2, inclined at an angle φ_{max} to the sample normal.

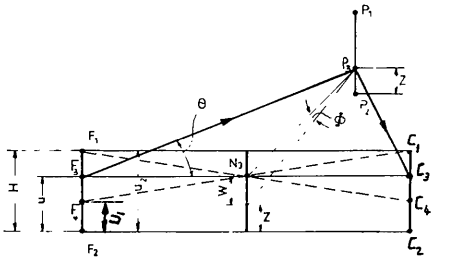

Fig. 2. Three-dimensional diffractometer geometry illustrating the definition of the probability function $f(\varphi)$.

Table 1. *Integration limits in the definition of the probability function* $f(\varphi)$

$\sin\varphi$	Z_1	Z_2	U_1	U_2
$\sin\varphi \le \sin\varphi_{max}/2$	0	$H/2-W$	0	$2(H+W)$*
$\sin\varphi \le \sin\varphi_{max}/2$	$H/2-W$	$H-W$	$2(H+W)-H$	H
$\sin\varphi \le \sin\varphi_{max}/2$	0	$H-W$	$2(H+W)-H$	H

* $W=(R\sin\theta)\sin\varphi$.

plane makes an angle φ with the focusing plane (Fig. 2). An incident ray from point F_3 of the focus (coordinate U) is reflected to the point C_3 of the detector slit. X-rays from other points of the focus will be diffracted by the same crystallite and contribute to the integrated intensity, provided they arrive at the detector slit anywhere between C_1 and C_2. Let us calculate the effective length of the focal line for the particular arrangement (coordinate Z and angle φ) of Fig. 2. These parameters will be invariant if we rotate F_3C_3 around the pole P_3N_3. Two extreme positions of this line F_4C_1 and F_1C_4 are defined by the edge points of the focus F_1 and the detector slit C_1. Thus, we can determine the lower U_1 and upper U_2 limits of the variation of the emitting point on the focus line. It is clear from Fig. 2 that $U_2=H$ and

$$U_1 = H-2[H-(Z+W)] = 2(Z+W)-H,$$

where $W\simeq(R\sin\theta)\sin\varphi$. These limits are correct for any Z if

$$W \ge H/2 \quad (\text{or } \sin\varphi \ge \sin\varphi_{max}/2)$$

and for $Z \ge H/2-W$ if

$$W \le H/2 \quad (\text{or } \sin\varphi \le \sin\varphi_{max}/2).$$

However, for small $Z \le H/2-W$ and $W \le H/2$ (or $\sin\varphi \le \sin\varphi_{max}/2$), edge points F_2 and C_2 will define the extreme positions of the F_3C_3 line, and the effective length of the focus line is confined between $U_1=0$ and $U_2=2(Z+W)$. In order to define the probability function for the normals $f(\varphi)$, we must account for all possible situations in which a particle with pole orientation φ diffracts X-rays into the receiving slit. In other words, we have to integrate over the length of both the focal spot and the specimen. Coordinate Z always varies between $Z=0$ and $Z=H-W$ (Fig. 2).

Thus, the probability function is defined as

$$f(\varphi) = \int_{z_1}^{z_2} dZ/H \int_{U_1}^{U_2} dU/H, \qquad (6)$$

where the integration limits are given in Table 1. Integration leads to the following expressions

$$f(\varphi) = 1/2-[\sin\varphi/(\sin\varphi_{max})]^2 \quad \text{if } 0 \le \sin\varphi \le \sin\varphi_{max}/2,$$
$$f(\varphi) = (1-\sin\varphi/\sin\varphi_{max})^2 \quad \text{if } \sin\varphi_{max}/2 \le \sin\varphi \le \sin\varphi_{max}. \qquad (7)$$

For $\varphi_{max}<30°$ it might be supposed that $\sin\varphi\simeq\varphi$, and (7) may be replaced by

$$f(\varphi) = 1/2-(\varphi/\varphi_{max})^2 \quad \text{if } 0 \le \varphi \le \varphi_{max}/2,$$
$$f(\varphi) = [1-(\varphi/\varphi_{max})]^2 \quad \text{if } \varphi_{max}/2 \le \varphi \le \varphi_{max}. \qquad (8)$$

In fact, (7) and (8) produce very similar probability functions even for greater φ angles, as can be seen from Fig. 3.

In contemporary diffractometers the axial divergence is usually limited by two sets of Soller slits. The action of this assembly is defined mainly by its angular divergence δ - the ratio of the distance between adjacent plates to the length of the assembly. If we extend the length of the Soller slits to be equal to the goniometer radius and retain the same divergence, then the focal spot, the specimen and the detector slit will be divided into parts of δR. Thus, in respect of the axial divergence and the distribution of correctly oriented particles, a diffractometer with two sets of Soller slits is equivalent to one without Soller slits but with a shorter axial length of components $H=R\delta$. Consequently, the maximum deviation of the normals is

$$\varphi_{max} = \arcsin(\delta/\sin\theta). \qquad (9)$$

After establishing the probability function $f(\varphi)$ we can extend (2) to the case of a diffractometer with a substantial axial divergence of incident and diffracted beams:

$$I = K_0QV \int_0^{\varphi_{max}} P(\varphi)f(\varphi)\,d\varphi. \qquad (10)$$

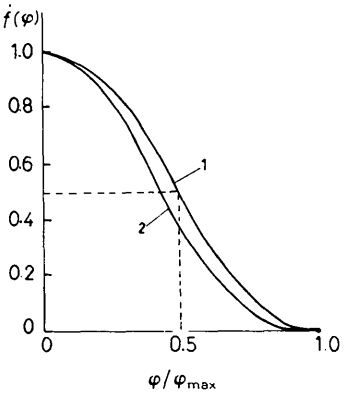

Fig. 3. Probability function $f(\varphi)$. (1) Simplified form (8); (2) precise form (7) for $\varphi_{max}=60°$.

P_0 from (2) is simply the pole density at $\varphi = 0$, and (10) accounts for the number of properly oriented crystallites and replaces the product $P_0 S_p$ of (2).

Theoretically, the maximum inclination of normals φ_{max} may approach 90°. However, high φ_{max} angles occur at low Bragg angles when peak broadening due to axial divergence of the primary and diffracted beam makes accurate measurement of the integrated intensity difficult. If $2\beta_0$ is the minimum practical diffractometer setting, then the following constraint will be imposed on φ_{max} (Fig. 1):

$$\varphi_{max} \leq \arctan (H/R \sin \beta_0);$$

if, for example, $2\beta_0 = 3°$, then $\varphi_{max} < 60°$ for various diffractometer arrangements.

Discussion

The significance of (10) compared with the conventional equation (2) depends on the relative width of the pole distribution functions and of the probability function $f(\varphi)$. Equation (2) holds when the pole distribution width is much greater than the angle φ_{max}; *i.e.* the variation of $P(\varphi)$ is small within the angular range $0 \leq \varphi \leq \varphi_{max}$. We start with a random sample $[P(\varphi) = 1]$. Integration in (10) with the probability function in the form (8) leads to

$$I = K_0 Q V \varphi_{max}, \tag{11}$$

where $\varphi_{max} = \delta/\sin\theta$ and, combining the constant instrumental factor δ with the scale factor constant K_0, we in fact recover the usual 'powder' supplement to the Lorentz factor $S_p = (\sin\theta)^{-1}$. However, if φ_{max} exceeds 30°, the precise probability function must be applied in the form (7). The integration in (10) can be performed in this case also and results in S_p values slightly greater than $1/\sin\theta$. For a diffractometer with two sets of Soller slits with divergence $\simeq 2°$, the discrepancy is ~5% for $2\theta = 5°$ and drops to zero at $2\theta = 10°$.

In another extreme case of perfect preferred orientation (the single-crystal case), $P(\varphi)$ may be regarded as a δ function and integration in (10) will produce a constant (θ-independent) term, giving the (obvious) value $S_p = 1$.

The intermediate cases are those of strong orientation and/or broad probability function $f(\varphi)$. Owing to the great increase in φ_{max} towards low Bragg angles, the practical examples are found among materials giving low-angle reflections of which clay minerals are typical. Usual diffractometric practice is to prepare oriented clay mounts. The 00l (basal) reflections are found at scattering angles from 4–5°, *i.e.* in the range where $f(\varphi)$ is especially broad. We have recently measured orientation functions for various clay mounts (Zevin & Viaene, 1990) and found that in this case as in many others (Lippmann, 1970; Taylor & Norrish, 1966; Reynolds, 1986) the orientation function can be fairly well approximated by the Gaussian curve

$$P = P_0 \exp(-\varphi^2/2\sigma^2). \tag{12}$$

P_0 from this equation is defined by normalization (4). Assuming $\sin\varphi \simeq \varphi - \varphi^3/6$, we obtain

$$P_0 = [\sigma^2(1 - \sigma^2/3)]^{-1}, \tag{13}$$

which is valid within a few percent for $\sigma < 30°$.

Although the real $P(\varphi)$ function usually decays more slowly than the Gaussian curve, the difference is almost insignificant in the integration of (10).

The standard deviation σ [(12)] for various clay mounts varies from 10 to 25°. Integration in (10) with the Gaussian orientation function (12) and the simplified probability function (8) leads to

$$I = K_0 Q V P_0 U, \tag{14}$$

where

$$\begin{aligned} U = \sigma\sqrt{2\pi}\{&[1 + (\sigma/\varphi_{max})^2] \operatorname{erf}(\varphi_{max}/\sqrt{2}\,\sigma) \\ &- [1/2 + 2(\sigma/\varphi_{max})^2] \operatorname{erf}(\varphi_{max}/2\sqrt{2}\sigma) \\ &+ (2/\sqrt{2\pi})(\sigma/\varphi_{max}) \\ &\times [\exp(-\varphi_{max}^2/2\sigma^2) - \exp(-\varphi_{max}^2/8\sigma^2)]\}, \end{aligned}$$

where the error function erf (x) is defined as

$$\operatorname{erf}(x) = (2/\sqrt{\pi}) \int_0^x \exp(-t^2)\, dt,$$

and P_0 is defined in (13).

If necessary, integration with the precise frequency function (7) could only be performed numerically. However, only small deviations from the approximate equation (14) would be anticipated due to the closeness of the two forms (Fig. 3).

The term U actually bears the supplementary powder Lorentz factor which may thus be represented as

$$S_p = CU, \tag{15}$$

where C is the scaling S_p factor.

The scaling is easily achieved given that at $\theta = 90°$, $S_p = 1$ for randomly oriented powder samples as well as oriented samples. [The latter is always confined between $S_p = (\sin\theta)^{-1}$ for a randomly oriented powder and $S_p = 1$ for single crystal.] For $\theta = 90°$, $\varphi_{max} = \delta$ [(9)] is much less than σ, even for sharp preferred orientation. Calculation of U on this assumption leads to $U_{max} = \varphi_{max}/2 = \delta/2$.

Thus, the scaling factor from (15), $C = 2/\delta$ and the 'powder' supplement to the Lorentz factor is calculated by

$$S_p = 2U/\delta,$$

where U is defined in (13).

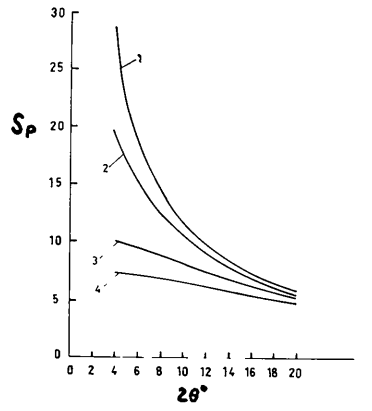

(*a*)

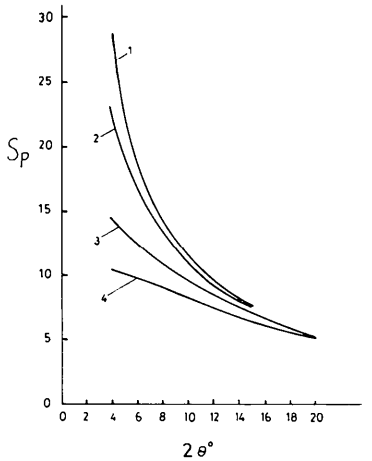

(*b*)

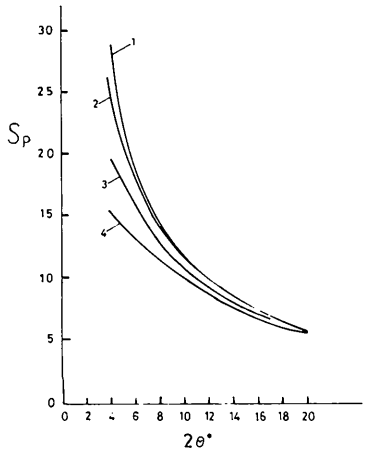

(*c*)

Fig. 4. Lorentz factor for oriented samples. (*a*) Standard deviation of orientation function $\sigma = 10°$; (*b*) $\sigma = 15°$; (*c*) $\sigma = 25°$; (1) $S_p = 1/\sin\theta$ curve; (2) diffractometer with two sets of Soller slits $\delta = 1°$; (3) diffractometer with two sets of Soller slits $\delta = 2{\cdot}3°$; (4) diffractometer without two sets of Soller slits, $H = 10$, $R = 173$ mm.

The values of S_p were calculated for various instrumental arrangements and three different levels of preferred orientation - sharp ($\sigma = 10°$), medium ($\sigma = 15°$) and relatively low ($\sigma = 25°$). The results are presented graphically in Fig. 4. The regular S_p powder factor $(\sin\theta)^{-1}$ is also shown in this figure. The deviation from the $(\sin\theta)^{-1}$ curve is indeed significant. However, this effect is confined to the range of scattering angles $2\theta < 20°$. As would be expected, the deviation from $S_p = (\sin\theta)^{-1}$ is especially significant for sharp texture and the high degree of integration achieved in diffractometers without Soller slits. However, even in the conventional diffractometer with two sets of moderate Soller slits ($\delta = 2{\cdot}3°$, Philips PW1050 goniometer), the effect is rather pronounced even for mild texture ($\delta = 25°$) at scattering angles lower than 10°. Thus, we define conditions under which substantial instrumental integration over the pole distribution takes place. If this is the case, the intensity correction for preferred orientation should be made by (10) rather than by the simpler equation (2).

Implementation of (10), of course, requires a knowledge of the pole orientation function $P(\varphi)$ and the angle of maximal pole deviation φ_{max}. The latter is derived from known experimental arrangements, for example, from (5) or (9). The orientation function $P(\varphi)$ requires special consideration. Parameters of this function are usually recovered as a by-product of Rietveld structure refinement by powder diffraction data. As is known, an orientation function may be used for intensity corrections in subsequent cycles of refinement, according to procedures outlined in this work. Integration in (10) might, of course, also be done numerically and not necessarily analytically as was shown in this paper. For strongly oriented samples like oriented clay mounts, the orientation function must be evaluated by conventional methods of texture analysis.

References

ALEXANDER, L., KLUG, H. P. & KUMMER, E. (1948). *J. Appl. Phys.* **19**, 742-753.

AZAROFF, L. (1968). *Elements of X-ray Crystallography*, p. 202. New York: McGraw Hill.

DOLLASE, W. A. (1986). *J. Appl. Cryst.* **19**, 267-272.

KHEIKER, D. M. & ZEVIN, L. S. (1963). *Ind. Lab. (USSR)*, **29**, 168-173.

LIPPMANN, F. (1970). *Contrib. Mineral. Petrol.* **25**, 77-94.

REYNOLDS, R. (1986). *Clays Clay Miner.* **34**, 359-367.

ROE, R. J. & KRIGBAUM, W. R. (1964). *J. Chem. Phys.* **40**, 2608-2615.

STURM, E. & LODDING, W. (1968). *Acta Cryst.* **24**, 650-653.

TAYLOR, R. M. & NORRISH, K. (1966). *Clay Miner.* **6**, 127-142.

WOLFF, P. M. DE (1958). *Appl. Sci. Res. Sect. B*, pp. 102-107.

ZEVIN, L. & VIAENE, W. (1990). In the press.